

Numerical Study of the Orographic Forcing of Heavy Precipitation during MAP IOP-2B

SEN CHIAO

Division of Engineering and Applied Sciences, Harvard University, Cambridge, Massachusetts

YUH-LANG LIN AND MICHAEL L. KAPLAN

Department of Marine, Earth and Atmospheric Sciences, North Carolina State University, Raleigh, North Carolina

(Manuscript received 10 October 2003, in final form 15 March 2004)

ABSTRACT

This paper investigates the local circulation associated with a heavy orographic rainfall event during 19–21 September 1999 [Mesoscale Alpine Programme Intensive Observing Period 2B (MAP IOP-2B)]. This event was simulated with a 5-km horizontal grid spacing using the fifth-generation Pennsylvania State University–NCAR Mesoscale Model (MM5). The MM5 simulation reproduced the basic features such as the timing and location of the deep trough and the associated precipitation evolution, though the total amount of precipitation is slightly higher than that measured by rain gauges (~30% in 24 h). The near-surface flow was dominated by an easterly jet originally from the Adriatic Sea and a southerly jet from the Gulf of Genoa. A significant westward turning occurred when the southerly flow approached the south side of the Alps. This deflection was caused by boundary layer friction and rotation, as well as mountain blocking effects. Flow was generally from the south above the surface. Precipitation was mainly concentrated on the windward slopes, especially near the Lago Maggiore region. Sensitivity experiments have been conducted to investigate the effects of upstream orography, the western flank of the Alps, boundary layer friction, and horizontal resolution. The results indicate that precipitation distribution and amount over the southern upslope region of the Alps were not directly related to either the coastal Apennine Mountains or the west flank of the Alps. The boundary layer friction reduces the total amount and alters the distribution of rainfall by weakening the wind near the surface. The 1.67-km horizontal grid spacing simulation indicates that heavy rainfall tended to be concentrated in the vicinity of individual mountain peaks. The total amount of rainfall was overpredicted along the windward slopes because of the strong upward motion that occurred on the upslope of the barrier. The results indicate the importance of dynamical forcing associated with upslope-induced and near-surface horizontal velocity convergence-induced vertical motion, which increases rapidly as horizontal resolution increases.

1. Introduction

A heavy orographic rainfall event occurred on 19–20 September 1999 during the Mesoscale Alpine Programme (MAP; Bougeault et al. 2001) Intensive Observing Period 2B (IOP-2B) when a deep trough propagated eastward through the Alps. The 24-h accumulated rainfall exceeded 250 mm locally. The heavy rain was concentrated on the windward slopes of the Alps, and in the Lago Maggiore target area (LMTA). Similar synoptic conditions and amounts of precipitation comparable to this event were recorded in the Piedmont flood event in November 1994, in which the southerly low-level jet, associated with the deep trough, evaporated moisture from the sea and advected it into the southern slopes of the Alps (e.g., Buzzi et al. 1998; Buzzi and Foschini 2000). A detailed description of the IOP-2B event was

presented by Lin et al. (2001b) and Asencio et al. (2003). Synthesis of the papers describing orographic rainfall events observed during MAP indicates that orographic rainfall over Alpine regions occurs under a variety of conditions (e.g., Bougeault et al. 2001; Houze et al. 2000; Smull et al. 2000; Steiner et al. 2000). Additionally, one piece of evidence suggesting that orographically induced circulations may play a role in heavy rainfall events is that the precipitation climatology over the Alps is not uniformly distributed but instead is distributed along the Alpine foothills and the shielding of the inner-Alpine valleys (e.g., Frei and Schär 1998). This study was stimulated by the fact that the precipitation was concentrated over the windward slopes around the Lago Maggiore region with a long duration in this event. Although many studies have demonstrated how the airstream moves past terrain features and what synoptic-scale conditions are favorable for orographic rainfall, it is important to understand the precise mechanisms that lead to the formation, distribution, and persistence over many hours of this type of orographic precipitation.

Corresponding author address: Sen Chiao, Harvard University, 29 Oxford Street, Pierce Hall 110-I, Cambridge, MA 02138.
E-mail: s.chiao@yahoo.com

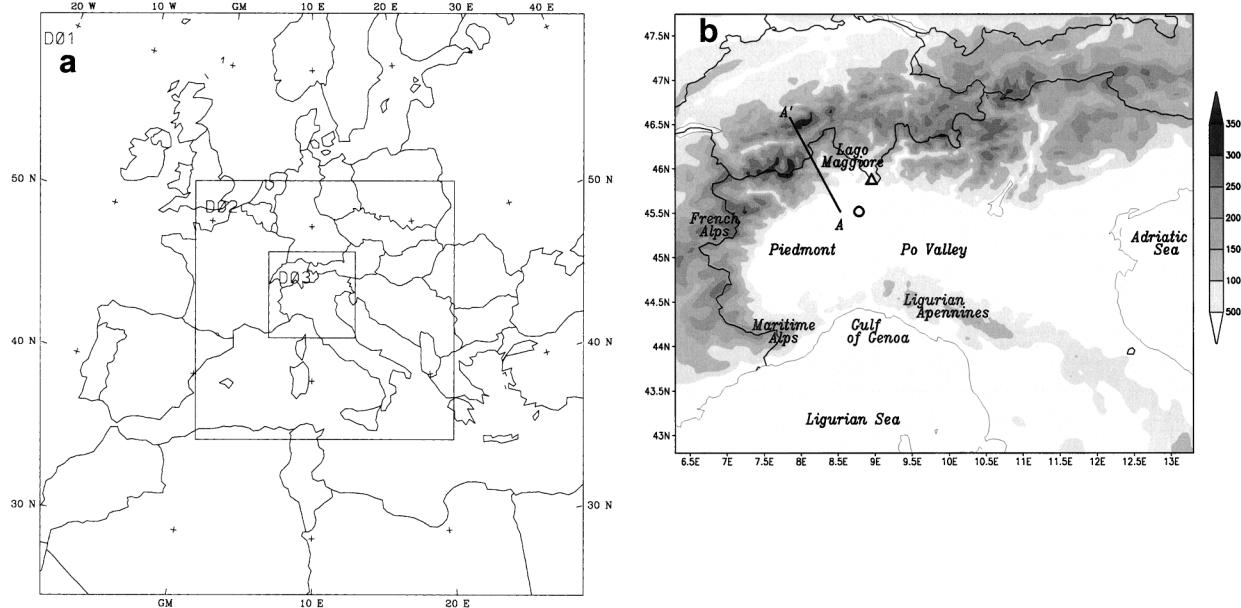


FIG. 1. (a) Domains for the numerical simulations used in this study. The grid increments for the three nested meshes are 45, 15, and 5 km, respectively. (b) Terrain (every 500 m) used for the 5-km domain CTRL. The solid line AA' represents the orientation of the x - z cross section in subsequent analyses. The triangle (Δ) and circle (\circ) represent the Monte Lema radar and wind profiler at Lonate.

Recent research (Buzzi and Foschini 2000) pointed out that orographic precipitation is generated by different mesoscale features associated with the interaction with topography, such as a moist low-level jet (LLJ) and near-barrier convergence zones. As a matter of fact, the orographic rainfall over the southern Alpine slopes often starts in the Lago Maggiore region when a moist LLJ flows from the Mediterranean. The strong influence of the Alps on the flow has also been demonstrated in the numerical work of Chen and Lin (2001). They concluded that a relatively large amount of rainfall can be produced over the upwind slope under the presence of an impinging LLJ. In addition, idealized experiments by Rotunno and Ferretti (2001) show that in the 1994 Piedmont heavy rainfall event, the western moist part of the airstream (saturated) flows over the mountains, while the eastern drier branch (unsaturated) is deflected westward around the obstacle. Thus, the convergence of air is produced between the airstreams, and heavy precipitation is produced. The influence of terrain on the flow and precipitation has also been demonstrated in the idealized simulation by Schneidereit and Schär (2000). They hypothesized that the Coriolis effect and a pronounced moist low-level jet provided a suitable environment for heavy condensation and precipitation.

A previous numerical study by Buzzi et al. (1998) has revealed that orographic rainfall would be strongly reduced as the height of the upstream mountains (i.e., Ligurian Apennines) and western flank of the Alps (i.e., French Alps) were reduced (Fig. 1b). They concluded that the lack of the orographic lifting would change the condensation, therefore resulting in reduced orographic precipitation. Stein (2002) also pointed out that if the

surrounding mountains are removed (i.e., Alps alone), the accumulated rain is less than 4 mm in a 12-h simulation. It is worth noting that simulations in Buzzi et al. (1998) and Stein (2002) were conducted with rather coarse 30- and 10-km resolutions, respectively. It appears that local circulations as well as the rainfall distributions in either the upstream mountains or western flank of the Alps are quite complicated and need further investigation. In this study, we focus on finescale simulations to understand the effects of the Ligurian Apennines and French Alps on local circulation as well as rainfall distribution.

The IOP-2B case provides an excellent opportunity to investigate how the orographic effects on moist flows can lead to heavy precipitation. The aim of this study is to advance fundamental knowledge of the interaction between orographically induced local circulations and precipitation processes over the Alpine mountain ranges. This purpose will require that we validate the mesoscale model performance in simulating precipitation over the regions of complex topography. The validating analysis is based on the data collected from the MAP field experiment, which includes special sounding ascents, surface data, radar observations, and rain gauge observations. Fine-resolution simulation (e.g., $\delta x = 5$ and 1.67 km) results will be used as a tool to create a mesoscale four-dimensionally consistent dataset describing the initiation of and subsequent evolution of orographic precipitation. The numerical model and experiment design are described in section 2. A general description of the spatial structure and temporal evolution of precipitation during MAP IOP-2B using the observed precipitation dataset and radar imagery are

TABLE 1. Summary of numerical experiments.

Experiment	Topography	Condition
CTRL	Real	—
NFRC	Real	No PBL forcing
NAPN	No Ligurian Apennines	—
NWAP	No French Alps	—
FALP	Real	$\Delta x = 1.67 \text{ km}$

discussed in section 3. The verification of the control simulation results is presented in section 4, while the sensitivity tests are discussed in section 5. Section 6 presents the conclusions.

2. Model description and design of numerical experiments

Numerical simulations were performed by using the fifth-generation Pennsylvania State University–National Center for Atmospheric Research (PSU–NCAR) Mesoscale Model (MM5; Grell et al. 1994). Three nested domains were constructed with the grid spacing of 45-, 15-, and 5-km horizontal resolutions, respectively. The corresponding numbers of grid points are 91×85 , 121×121 , and 121×121 . The model top is located at the 50-hPa level. Time steps of 90, 30, and 10 s were used in these nested grid simulations, respectively. The 45-km resolution domain covered Europe, and the 5-km domain was concentrated in northern Italy (Fig. 1a). Several options are available in the model for parameterization schemes of physical processes. The planetary boundary layer (PBL) scheme used in this study is the Blackadar high-resolution PBL scheme (Zhang and Anthes 1982). The atmospheric radiation scheme, described by Dudhia (1989), accounts for longwave and shortwave transfers and interactions within the atmosphere, clouds, and the surface. Precipitation is produced from both grid-scale condensation and convection. Grid-scale precipitation is determined from an explicit moisture scheme of Lin et al. (1983) that includes graupel. The Kain–Fritsch (1993) scheme was adopted for the cumulus parameterization. Klemp and Durran's (1983) upper-radiative boundary condition was applied in order to prevent gravity waves from being reflected from the model top. In the control experiment (CTRL; see Table 1 for a list of numerical experiments), the model contains 1-km horizontal resolution terrain data. The terrain data for the third (i.e., finest) grid mesh of $\Delta x = 5 \text{ km}$ is shown in Fig. 1b. The model topography data are representative of the complex local topographic features, with several mountain peaks of the Alps higher than 3500 m.

In order to examine the relative roles of upstream topography on the formation of orographic precipitation over the Lago Maggiore region, we conducted several experiments in an attempt to isolate their effects on local circulations, which affected the formation of orographic

precipitation. To test the effect of upstream mountains, we performed a simulation without the Ligurian Apennines as well as without the mountains of Corsica and Sardinia (NAPN) on 15- and 5-km domains, while keeping everything else identical to the CTRL. The Ligurian Apennines topographic feature is very similar to the arc-shaped barrier-like obstacle of the Alps. The control simulation's upstream topography includes the Apennines and the mountains on Corsica and Sardinia. In addition to the NAPN, in order to better gauge the initiation of orographic rainfall, we carried out an experiment in which the Maritime Alps (i.e., French Alps) were set to be flat from 43° to 45°N , while keeping everything else identical to the NAPN. Thus, the mountain range was very similar to an east–west elongated ridge. This experiment is denoted by NWAP. In order to test the frictional effects, another experiment (NFRC) with a free-slip lower boundary was also conducted. In addition, we also conduct a 1.67-km horizontal grid spacing simulation using a one-way nested approach. Detailed discussions about these sensitivity experiments are presented in section 5.

All the simulations used the same initial and lateral boundary conditions, which are generated from the National Centers for Environmental Prediction–National Center for Atmospheric Research (NCEP–NCAR) reanalysis (Kalnay et al. 1996) with $2.5^\circ \times 2.5^\circ$ resolution, which also included snow cover and sea surface temperature. The first-guess fields interpolated from the reanalysis are then enhanced by the blending in of the rawinsonde, surface observational data using the Cressman (1959) analysis technique to introduce mesoscale features. Time-dependent lateral boundary conditions are provided at 12-h intervals. A total of 46 unequally spaced levels in the vertical, with the lowest model level beginning approximately 20 m above ground, are used. Forty-eight-hour simulations were run from 0000 UTC 19 September to 0000 UTC 21 September 1999. Our discussions are based on the results of the 5-km grid domain.

3. Observed local circulation and rainfall

In this section, a description of the observed mesoscale evolution of IOP-2B is presented, followed by an examination of the low-level local circulation induced by the Alps, and the spatial and temporal distribution of precipitation. The analysis is based on conventional data, visible satellite imagery, and high-resolution networks of Alpine countries' rain gauge datasets, including Italy, Austria, and Switzerland. These datasets and daily analyses are available at the MAP Data Center (e.g., Frei 1995; Frei and Häller 2001). While all the available observations were used, a limited number of observations are analyzed and presented here. The synoptic environment for IOP-2B was presented in Lin et al. (2001b). In addition, Houze et al. (2000) and Rotunno and Ferretti (2002) have analyzed the orographic

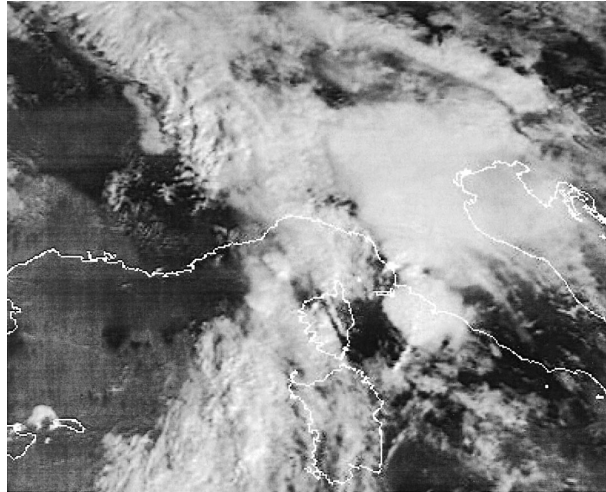


FIG. 2. European Organization for the Exploitation of Meteorological Satellites (EUMETSAT) image at 0900 UTC 20 Sep 1999.

rainfall associated with IOP-2B. However, their studies focused on the later development stage of IOP-2B. This study concentrates on the earlier mesoscale aspects of the orographic precipitation.

IOP-2B took place during 19–21 September 1999 when a trough swept into northern Italy and heavy rain was concentrated on the windward (southern) slopes of the Alps and in the Lago Maggiore region. During the IOP, a south-southwesterly LLJ was accompanied by the eastward-moving deep trough, which impinged on the Alps (see Lin et al. 2001). This LLJ serves as a contributor to the process that produces heavy orographic rainfall (e.g., Lin et al. 2001b). Figure 2 shows a visible satellite image from *Meteosat-6* rapid-scan data at 0900 UTC 20 September. The imagery indicates a large area of clouds south of the Alps in a wide band extending from the central Mediterranean northward through northern Italy and the Alps. The saturated scenario suggests that large-scale ascent was associated with the trough at that time and was manifested as a mesoscale precipitation shield that covered the south side of the Alps as well as the Lago Maggiore region. The 500-hPa height field from the European Centre for Medium-Range Weather Forecasts (ECMWF) 0.5° analysis data and the 850-hPa radiosonde observations from 1800 UTC 19 September to 1200 UTC 20 September at 6-h intervals are presented in Figs. 3a–d. During this period, the low-level flow is mainly from the south or southwest. The low-level wind increased when the trough moved into northern Italy. ECMWF 0.5° analyses also indicated that a moist flow orthogonal to the south side of the Alps at the 2-km level generally was from the south to southwest throughout the entire period of precipitation (Rotunno and Ferretti 2002).

The rainfall event in IOP-2B started with light rain around 1500 UTC 19 September, intensified during the night, and became more convective around 1000 UTC

20 September, especially on the southern slopes of the Alps. Doppler radar observations during this time period showed the presence of a precipitation shield located near the windward slopes of the Alps as well as in the Lago Maggiore region (e.g., Houze et al. 2000). There are major persistent and intense precipitation rates greater than 10 mm h^{-1} occurring over the south-facing slopes of the Alps in the Lago Maggiore region that last approximately 12 h (figure not shown).

The Cressman (1959) objective analysis approach has been used in analyzing hourly high-resolution networks of rain gauge data in this study. The distribution of rain gauge stations is fairly balanced over the analysis domain (see Frei 2004). Figure 4 shows the time sequence of 6-h accumulated analyzed rainfall during 1200 UTC 19 September to 1200 UTC 20 September. Beginning in the late afternoon of 19 September (local time), light rain initiated along the steep southward-facing slopes of the Maritime Alps and the southeastward-facing slopes of the Alps in between 45° and 46°N , that is, the concave topography area (Fig. 4a). From 1800 UTC 19 September 0000 UTC 20 September (Fig. 4b), the rain was located generally over the same location as depicted in Fig. 4a, but at a heavier rate. Some light rain was also recorded around the Piedmont area. Total rainfall amount increased, and the rainfall was more concentrated on the windward slopes from 0000 to 0600 UTC 20 September (Fig. 4c). As illustrated in Fig. 4c, some peak values of rainfall of 20 mm h^{-1} were observed over the Lago Maggiore region, Maritime Alps, and the Po Valley. In the afternoon (local time) of 20 September (i.e., 0600 to 1200 UTC), the precipitation area broadened on the windward slopes of the eastern side of the Alps and moved toward the east along with the trough (Fig. 4d). Light rain was still observed in the Lago Maggiore area at 1800 UTC 20 September. Note that because of the prolonged moderate–heavy rainfall period over the south side of the Alps as well as the Lago Maggiore area, the 24-h accumulated rain had exceeded 200 mm. In summary, the moist south to southwesterly flow associated with the trough/low pressure system was instrumental in producing heavy rainfall over the windward slope. The rain over the up-slope region of the Alps started around the concave area, and then migrated eastward along with the movement of the trough. The heavy rain over the Lago Maggiore area lasted approximately from 1500 UTC 19 September to 0000 UTC 21 September 1999.

4. Control simulation and comparison with observed analysis data

The 5-km resolution simulation was initialized at 0600 UTC 19 September 1999, which was about 12 h prior to the formation of heavy rainfall over the south side of Alps. This allows the prerainfall environment to be examined. The winds computed from the dual-Doppler radar data around 0900 UTC 20 September indicated

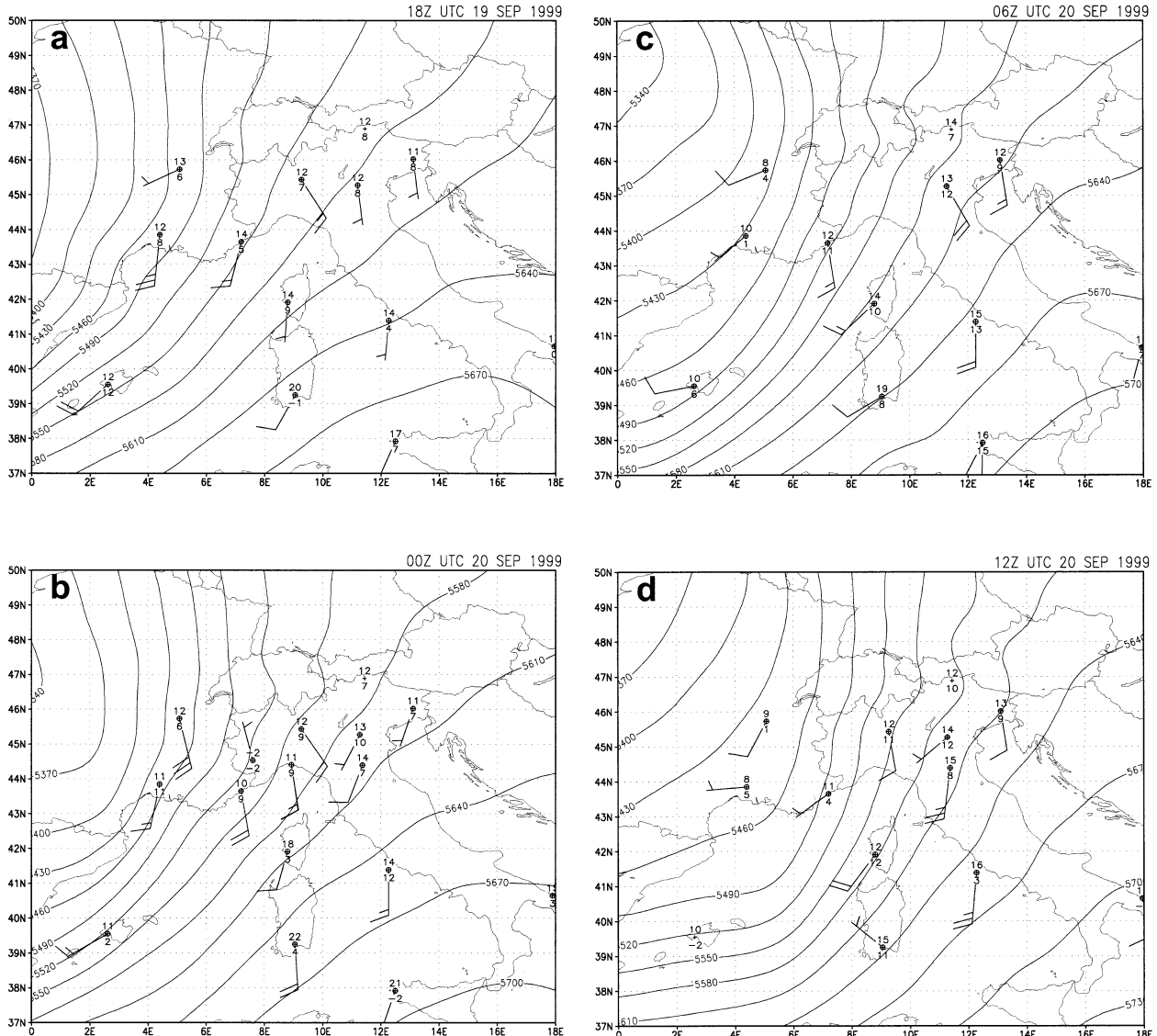


FIG. 3. Geopotential height analysis at 850 hPa at (a) 1800 UTC 19 Sep, (b) 0000, (c) 0600, and (d) 1200 UTC 20 Sep 1999. Available radiosonde data plotted using station model.

the flow into the Lago Maggiore region at the 2-km level was generally from the south, and the flow turned to the left as it approached the barrier (Fig. 5a). As the wind turned to be more southeasterly, it flowed nearly perpendicular to the southwest–northeast-oriented mountains on the western side of the Lago Maggiore region. The model was able to capture this low-level south to southeasterly flow, as well as the cyclonic turning near the Lago Maggiore region. The model-calculated radar reflectivity (~ 40 dBZ) was also consistent with those observed by the dual-Doppler radars (Fig. 5b).

Figure 6 shows the horizontal evolution of the simulated wind and convergence at the lowest model level ($\sigma = 0.995$) for a portion of the 5-km resolution domain from 1800 UTC 19 September to 1200 UTC 20 Sep-

tember at 6-h intervals. At 1800 UTC 19 September (Fig. 6a), a convergence zone was formed along the foothills on the western side of the Lago Maggiore area (i.e., concave area) in association with a weak south-easterly flow from the Adriatic Sea. The convergence zone was consistent with the observed rainfall area (Fig. 4a). By 0000 UTC 20 September (Fig. 6b), an unambiguously easterly jet had developed along the south side of the Alps, which is often referred to as a barrier jet. This barrier jet was formed by the westward turning of the low-level southeasterly flow as blocking allowed rotation effect to dominate low-level parcel dynamics. This westward turning is the result of the combined orographic blocking, Coriolis deflection, and boundary layer friction. The formation of this barrier jet is further discussed in section 5. The convergence zone persisted

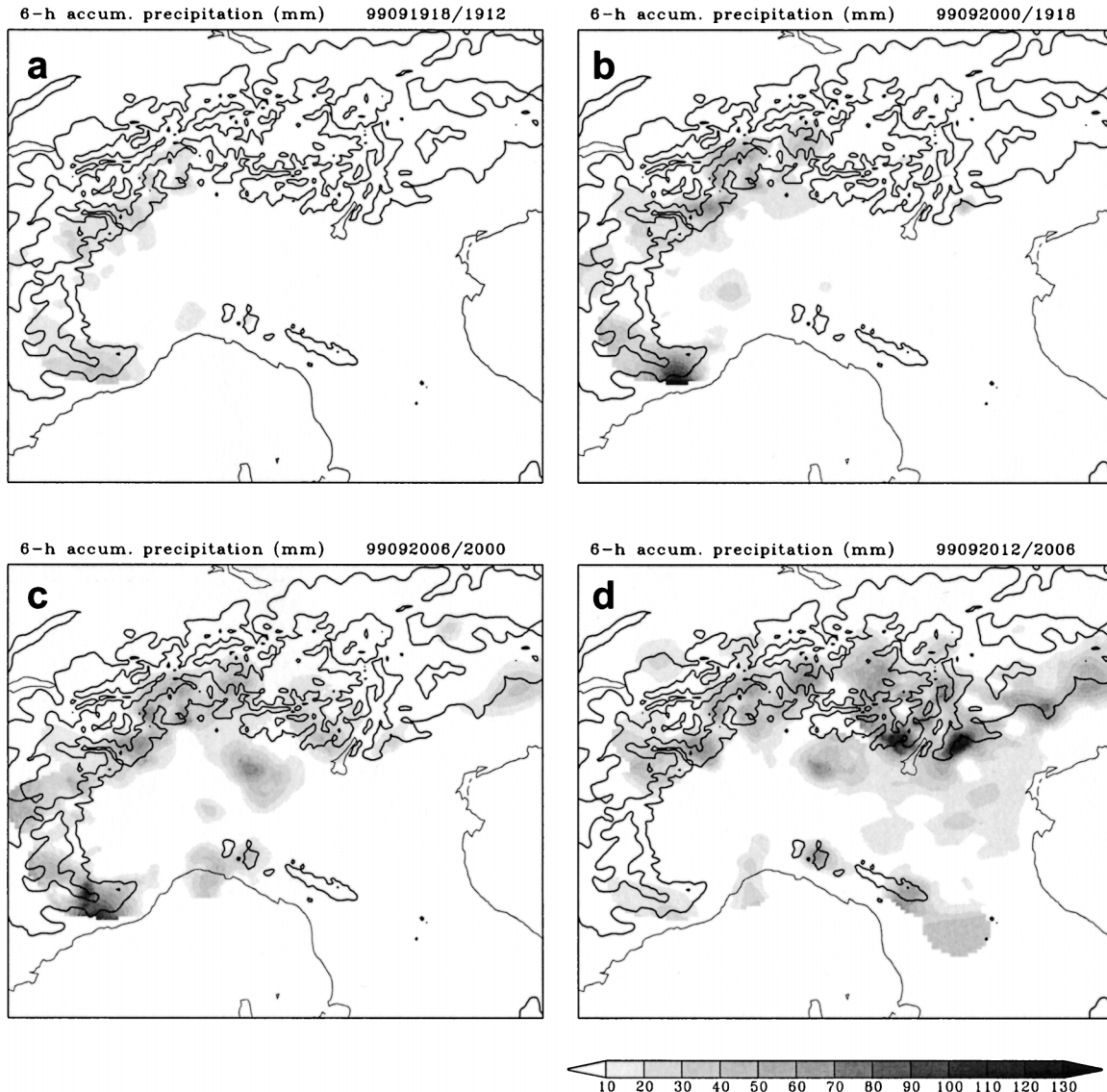


FIG. 4. Objectively analyzed 6-h accumulated rainfall (mm) ending at (a) 1800 UTC 19 Sep, (b) 0000, (c) 0600, and (d) 1200 UTC 20 Sep 1999.

near the concave area throughout this period. At 0600 UTC 20 September, the convergence had intensified along the southern slopes of the Alps (Fig. 6c), which was caused by the juxtapositioning of the intensified low-level southeasterly flow from the Ligurian Sea and the barrier jet. By 1200 UTC 20 September (Fig. 6d), there were several significant convergence zones along the mountain slopes, even though the trough had moved to the east. These convergence zones were consistent with the observed rainfall distribution at that time (Fig. 4d). A noteworthy feature is that a convergence zone also existed over the upslope region near the concave area throughout this period.

The model-simulated wind field, 850-hPa equivalent potential temperature (θ_e) field, and rainfall distribution

from 1200 UTC 19 September to 1200 UTC 20 September 1999 at 6-h intervals are presented in Fig. 7. Comparison of the simulated and observed winds at 1800 UTC 19 September (Figs. 7a and 3a) shows that the model has replicated the southerly flow along the Gulf of Genoa, and clearly shows the westward turning of the southerly flow near the south side of the Alps. Also, a high θ_e (~ 324 K) zone existed near the coastal area. The 6-h rainfall distribution was consistent with the observed analysis (Figs. 7a and 4a). Areas of light to moderate precipitation extended from the Maritime Alps to the western side of the Lago Maggiore area. During the next 6 h, the simulated rainfall is very similar to the observed analysis (Figs. 7b and 4b). The southerly flow had intensified in association with a moist tongue

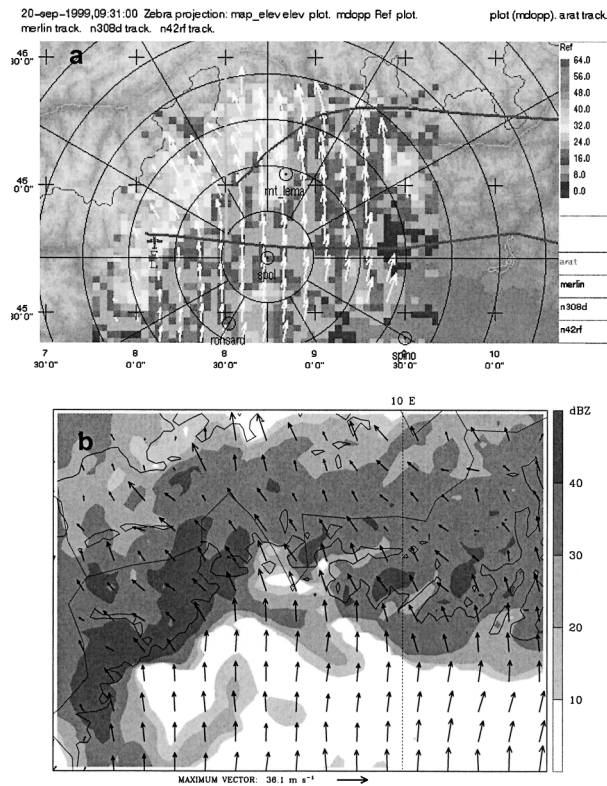


FIG. 5. Radar reflectivity and wind vectors at the 2-km level at 0900 UTC 20 Sep 1999: (a) S-Pol observed, (b) simulated from the CTRL 5-km-resolution domain.

impinging on the south side of the Alps at this time. The southerly flow near the foothills of the Alps as well as the Lago Maggiore area was deflected to the west. As mentioned earlier, this westward turning was caused by the mountain blocking as determined from sensitivity simulations to be presented later. Also, the 850-hPa wind field (Fig. 7a) differed from that at the surface level (Fig. 6b) due to the boundary layer forcing. More discussion of this phenomenon in a sensitivity experiment with no boundary layer friction is presented later. By 0600 UTC 20 September, the trough had reached northern Italy, which resulted in strong wind speed and higher θ_e over the Po River basin (e.g., 850 hPa). The simulated heavy rainfall occurred along the windward side of the Maritime Alps and the Ligurian Apennines, as well as the Lago Maggiore area (Fig. 7c). Compared with the observed rainfall during this period (Fig. 4c), the rainfall was overpredicted around the coastal areas and over the southern Alpine slopes by the model, but underpredicted at the southern tip of the Maritime Alps. The simulated wind shift around the Gulf of Genoa and Ligurian Sea is more than what was observed (Fig. 4c). This may be due, in part, to the strong surface fluxes over the Ligurian Sea in the numerical model as well as numerous other causes including imperfect initial data. In addition, the static stability profiles generated from the upstream soundings at Cagliari (southern tip of Sardinia) at dif-

ferent times, which are compared with the real soundings observed at the same location. The results are comparable (not shown).

By 1200 UTC 20 September, the synoptic analysis indicates that the trough moved to the eastern side of the Alps (not shown). As revealed by the 5-km domain simulation, the southwesterly low-level jet associated with the trough has also approached the same location (Fig. 7d). Also, a broad area of high θ_e (~ 328 K) in association with this trough existed over the Po Valley. The simulated rainfall distribution was generally consistent with observational analyses (Fig. 4d). Also, some heavy rainfall existed over the windward upslope regions, similar to those produced by small to moderate convective cells embedded in the broad-scale area of precipitation over the windward slopes (Houze et al. 2000). The rainfall distribution, by virtue of its location, also indicates that the low-level convergence is very effective in forcing the moist air upward and producing heavy precipitation. However, the rainfall was overpredicted on the western side of the Lago Maggiore region (i.e., the concave area) and the coastal areas. Sensitivity tests involving partially removing the orography in an area around the upstream mountains (i.e., Apennines), removing the western flank of the Alps (i.e., French Alps), and employing a finer-resolution simulation were performed to further investigate this issue, as discussed in the next section. Overall, the MM5 captured many of the salient features of this event, although the total amount of simulated precipitation is significantly higher ($\sim 30\%$ in 24 h) than observed. The similarity between simulated and observed precipitation in terms of pattern and timing suggests that the model has represented the physical processes, which are responsible for producing the precipitation, reasonably well.

To further document the evolving vertical structure of the simulated trough as it passed over northern Italy, Fig. 8 shows a cross section (AA') from the northwest to southeast direction. At 1800 UTC 19 September (Fig. 8a), the θ_e gradients parallel to the cross section were strong (particularly near the surface). There was a band of strong (~ 35 dBZ) convective echoes over the mountain upslope region, which is consistent with observations as well as the convergence zone. As the trough approached, precipitation intensity in this zone increased vertically, that is, up the mountain. It can be seen that strong upward motion on the windward slopes realized that potential instability ($\partial \theta_e / \partial z < 0$). An area of convection had increased to 40 dBZ over the lower windward slope during the past 6 h (Fig. 8b). By 0600 UTC 20 September, convection increased significantly over the windward slope. The simulated radar reflectivity clearly indicates the appearance of a strong convective echo as the trough moved over northern Italy (Fig. 8c). This echo is likely due to the orographically induced upward motion and the background lifting that combined to trigger strong convection in a potentially unstable layer. The simulated strong convective motion is

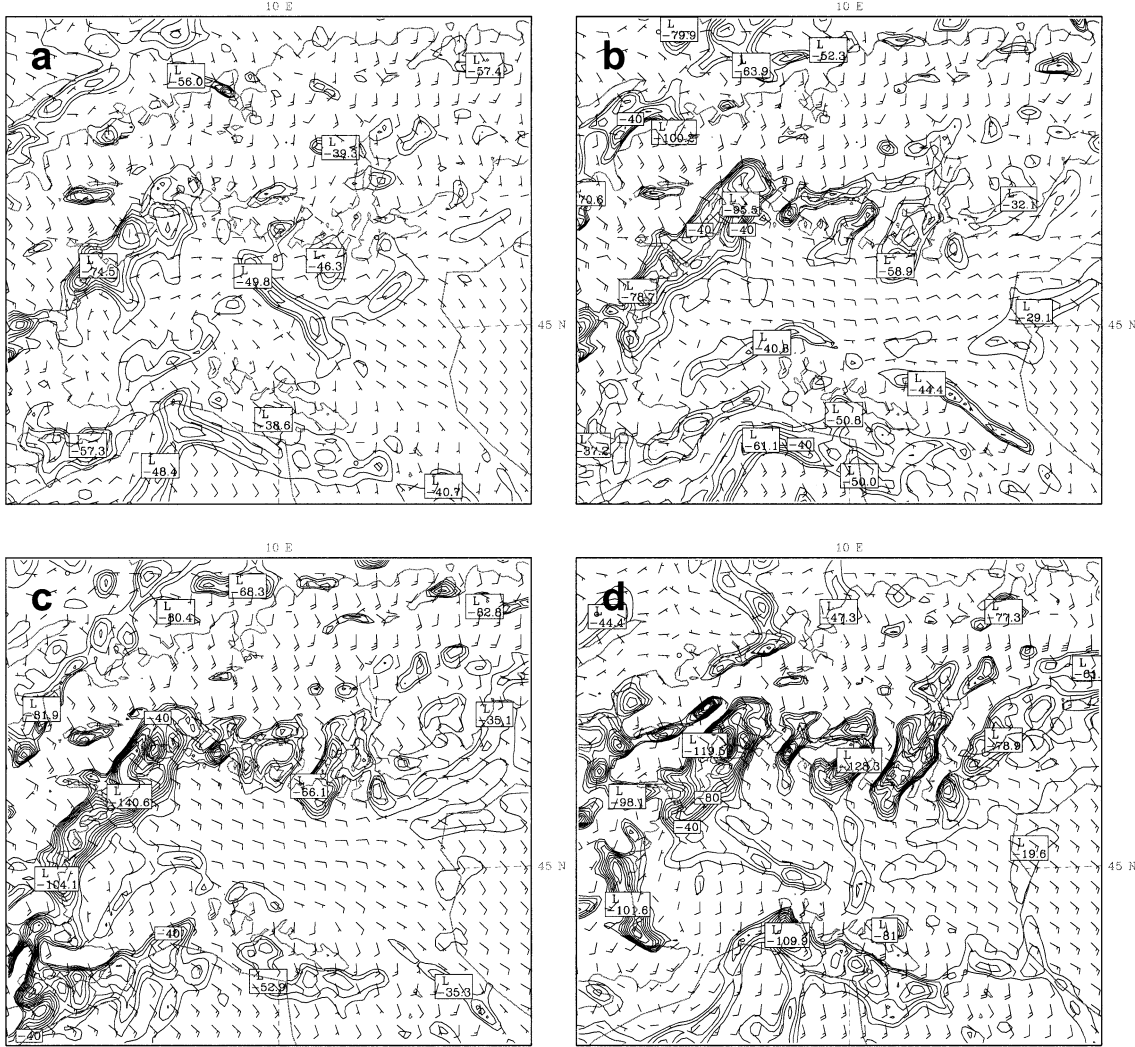


FIG. 6. Simulated surface level ($\sigma = 0.995$) convergence and winds (one full barb = 10 m s^{-1}) from the CTRL 5-km-resolution domain at (a) 1800 UTC 19 Sep, (b) 0000, (c) 0600, and (d) 1200 UTC 20 Sep 1999.

consistent with the observed analyses by S-band dual-polarized Doppler radar (S-pol; see Medina and Houze 2003). By 1200 UTC 20 September (Fig. 8d), the convection weakened as the trough moved to the eastern side of the Alps. The convective reflectivity structure over the mountain peaks still existed at this time.

5. Model sensitivity studies

An important objective of this study is to investigate the dynamical and physical processes, which are responsible for producing heavy orographic precipitation. The sensitivity simulations conducted in this study are designed to isolate effects on local circulations and orographic precipitation due to the Ligurian Apennine Mountains, western flank of the Alps (i.e., French Alps), PBL forcing, and small-scale features of the topography. Characteristics of these experiments are summarized in

Table 1. The topographic features of key importance to be investigated in these sensitivity experiments are shown in Fig. 9.

a. Effects of planetary boundary layer forcing

While it is widely recognized that the boundary layer can have important effects on flow over topography (e.g., Richard et al. 1989; Ölfsson and Bougeault 1997; Braun et al. 1999; Peng et al. 2001), few studies address the frictional effects on the local circulations in terms of the flow deflection and rainfall distribution. Therefore, an experiment with a free-slip lower boundary condition has been conducted. This experiment is the same as the CTRL, except the lower boundary condition is set to no friction (NFRC) and no planetary boundary layer fluxes are allowed (i.e., friction velocity, $U_* = 0$). When we turned off the boundary layer processes,

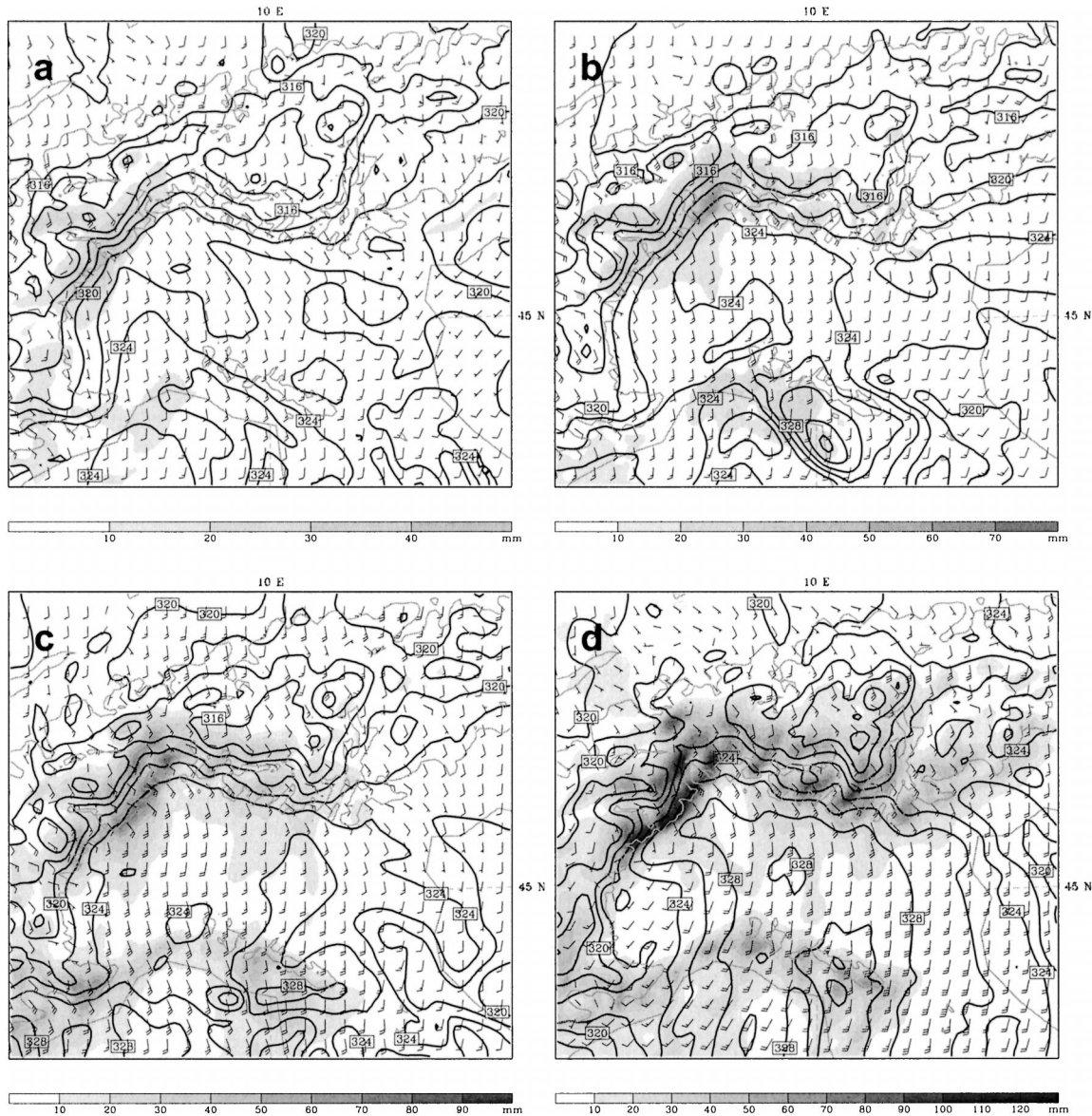


FIG. 7. Simulated 850-hPa winds (one full barb = 10 m s^{-1}), equivalent potential temperature (solid) every 3 K, and 6-h accumulated precipitation (shaded) for the 5-km resolution CTRL case ending at (a) 1800 UTC 19 Sep, (b) 0000, (c) 0600, and (d) 1200 UTC 20 Sep 1999.

we deactivated not only the surface friction effects but also thermal effects from the surface layer. Therefore, the boundary condition for the NFRC case is basically free slip and thermally insulated. However, the flow is not inviscid, because subgrid horizontal and vertical eddy diffusivities are allowed in the model (Chen et al. 1997). Figure 10 shows the 850-hPa wind fields, θ_e , and accumulated rainfall at 6-h intervals. As can be seen in Fig. 10a, valid at 1800 UTC 19 September, the absence of surface friction on the 6-h accumulated rainfall and wind field at 850 hPa are similar to the CTRL run (Fig. 7a). However, a low-level easterly jet is shown in the difference of NFRC – CTRL (Fig. 11a). By 0000 UTC

20 September (Fig. 10b), the flow at 850 hPa shows the westward turning of the southerly flow in the Po Valley. It was nearly perpendicular to the windward slope on the western side of Lago Maggiore area. Nevertheless, the wind fields at surface level indicate a southerly flow of $\sim 20 \text{ m s}^{-1}$ approaching the barrier and no westward turning occurred near the Alps or in the Po Valley, except a slight deflection, which occurred near the Lago Maggiore area (not shown). The surface-level wind difference of NFRC – CTRL also indicated that strong southwesterly wind existed in the Po Valley (Fig. 11b). Apparently, the lack of surface friction enhanced the magnitude of flow at this time. In other words, the sur-

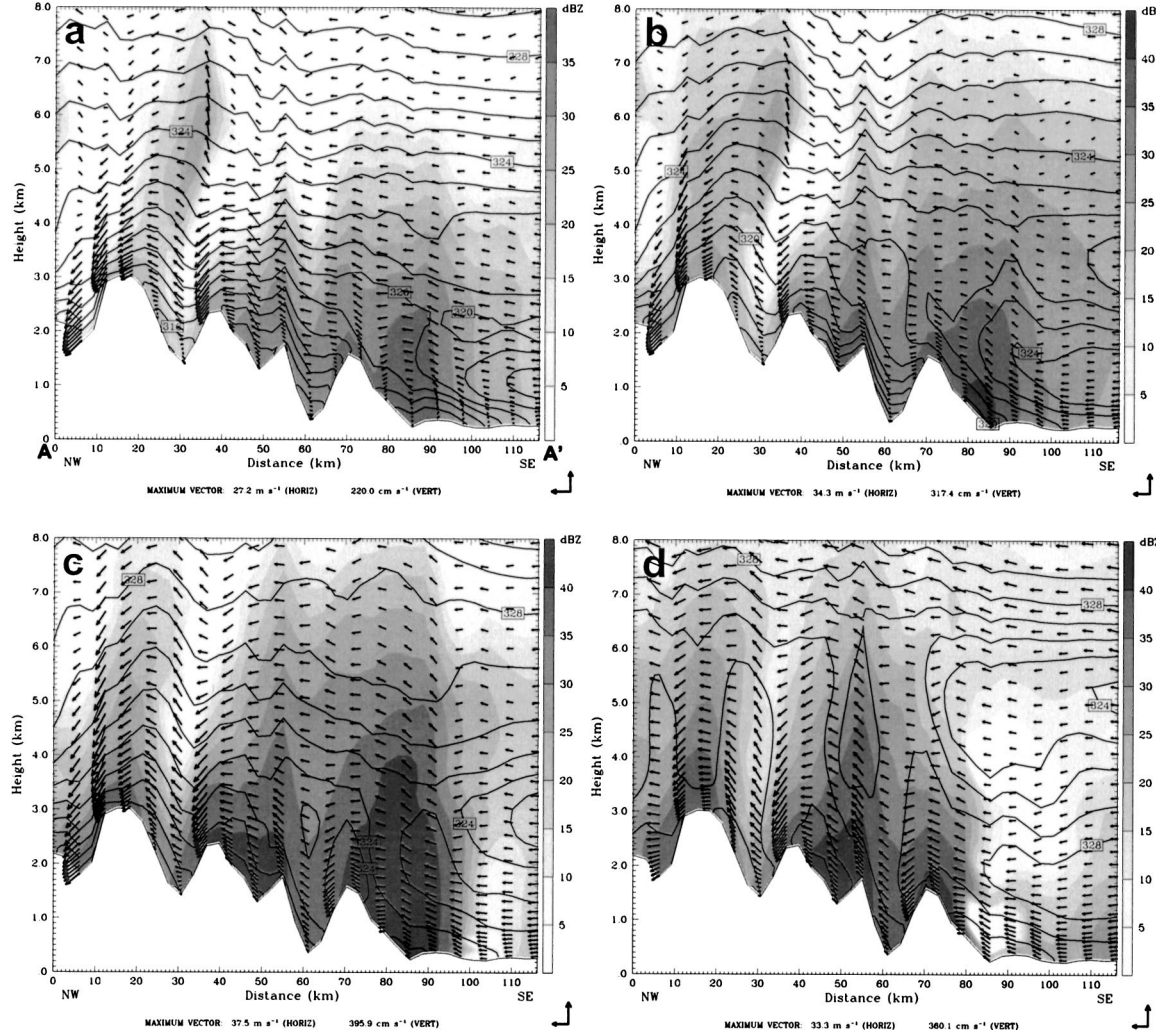


FIG. 8. Cross section AA' for the 5-km domain at (a) 1800 UTC 19 Sep, (b) 0000, (c) 0600, and (d) 1200 UTC 20 Sep 1999 showing equivalent potential temperature (solid every 1 K), model reflectivities (shaded), and the total circulation (vectors) in the cross section.

face friction acts to decelerate the inertial–advective component of the wind.

By 0600 UTC 20 September, broad-scale precipitation fell on the windward slopes as well as in the Po Valley in experiment NFRC (Fig. 10c). In addition, a significant downslope wind ($\sim 30 \text{ m s}^{-1}$) was simulated over the lee side of the Alps. The difference (NFRC – CTRL) of accumulated rainfall is shown in Fig. 11c. The rainfall over the Po Valley, compared to the CTRL run, was partly the result of the lower-level convergence due to the lack of surface friction (not shown). At 1200 UTC 20 September (Fig. 10d), the strong southerly flow of $\sim 25 \text{ m s}^{-1}$ associated with the eastward movement of the trough was one of the main features. A zone of substantial low-level convergence occurred in the Po Valley (not shown). The major difference in cases NFRC and CTRL is that there was a zone of rainfall extending from the Po Valley southeastward, which was associated with a convergence zone. This convergence zone was

caused by the decreased westward turning of the wind in the NFRC case. The 6-h accumulated rainfall in the NFRC run at this time is as much as 70 mm higher than the CTRL run in the Po Valley (Fig. 11d). However, the accumulated rainfall over the windward slopes of the Alps in NFRC is about 30 mm lower than the CTRL run (not shown). As anticipated, the wind field difference of (NFRC – CTRL) over the upslope region reveals that wind speeds were stronger in NFRC case. This indicates that the southerly flow in the NFRC case fell more in the regime of flow over the terrain barrier than that of flow around the terrain barrier (Smith and Grönås 1993; Schneidereit and Schär 2000). Thus, the accumulated precipitation is lower over the upslope region in NFRC than CTRL from the period of 0600 to 1200 UTC 20 September 1999.

Figure 12 shows a series cross sections (AA'; see Fig. 1b) to illustrate how the equivalent potential temperatures, wind, and radar reflectivity structures evolved dur-

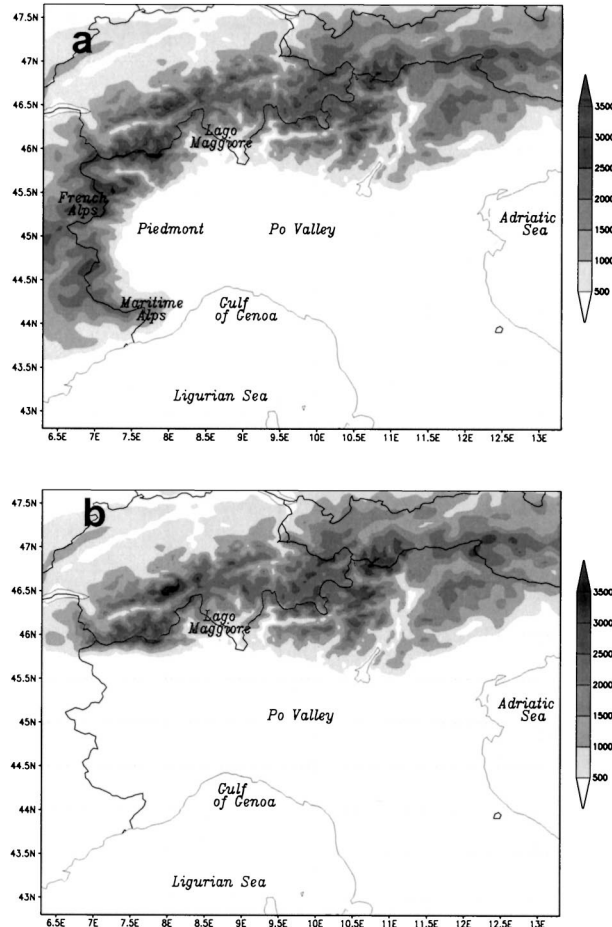


FIG. 9. Terrain features for (a) no upstream terrain (NAPN) and (b) no western flank of the Alps (NWAP).

ing the passage of the trough when there was no surface friction. By 0600 UTC 20 September, as the trough moved to the northern Italy (Fig. 12a), the vertical reflectivity structure shows convection (~ 35 dBZ) extending up to 3 km along the windward slopes. In contrast to the CTRL case, the convective echo structure appears to be much weaker in the NFRC case. Meanwhile, the equivalent potential temperature gradients were relatively weak (Fig. 8c). By 1200 UTC 20 September (Fig. 12b), the convection was strengthened, but not as deep as in the CTRL case 6 h earlier (Fig. 8c). It appears that the convection was shallower due to the lack of surface friction in terms of thermal mixing effects or reduced convective available potential energy due to cooler surface temperatures. Furthermore, it appears that the large-scale flow may have changed in the NFRC case, and the static stability in the cross section (Fig. 12a) aloft is much different than the CTRL case. The large differences in the PBL suggest the importance of fluxes upstream. In summary, without surface friction, there was less westward deflection of the low-level wind. In other words, the Coriolis effect was changed

implicitly by changing friction as inertial–advective flow was strengthened. Consequently, more flow over the mountains occurred and the upslope convection is shallower.

b. Effects of the upstream and concave topography

To test the effects of upstream mountains on the precipitation, a simulation (NAPN) without upstream topography (i.e., Ligurian Apennine Mountains) was performed on 15- and 5-km resolution domains, while keeping everything else identical to the control experiment. Figure 9a shows the topography on the 5-km resolution domain. From 1800 UTC 19 September to 0000 UTC 20 September, there was less westward deflection of the flow at 850 hPa in the NAPN case compared to the CTRL case (not shown). The flow near the Lago Maggiore area was about 10 to 15 m s $^{-1}$, and the 6-h accumulated rainfall distribution was also similar to the CTRL case (not shown). From 0600 to 1200 UTC 20 September (Fig. 13), strong convergence zones occurred around the Lago Maggiore area in association with the southeasterly low-level jet (~ 15 m s $^{-1}$). The strong low-level convergence zone was generally consistent with the precipitation over the upslope region of the Alps (Figs. 13c and 13d). In addition, the distribution of the θ_e gradients were still similar to those in the CTRL (Figs. 7c and 7d). In general, the simulated evolution of the local circulation is qualitatively similar to the CTRL (Figs. 6 and 7). However, a feature worthy of note is that a broad-scale area of rainfall (~ 20 mm in 6 h) fell on the Po Valley, which was caused by the absence of upstream mountain blocking (Figs. 13c and 13d). Evidence supporting this result was that in the CTRL case the precipitation on the windward slopes of the Ligurian Apennine Mountains was due to the coastal blocking, which results in the shallow convection along the windward slopes. In addition, this coastal blocking also suggested a rain shadow effect, which resulted from downslope wind as the southerly flow developed over the crest of the Ligurian Apennine Mountains. The rain shadow effect has also been found over California's coastal mountains (e.g., Ralph et al. 2003). In general, the rainfall distribution on the windward slopes of the south side of the Alps was not directly related to the Ligurian Apennine Mountains. The widespread rain in the Po Valley in the NAPN case corroborated the conclusions of Stein (2002), but in his case, relatively coarse model resolution (10 km) was used.

As discussed above, the model tends to overpredict the precipitation around the concave area as well as in the Lago Maggiore area in the CTRL case. Although it was partly due to the model-simulated low-level confluence in that area, the results also imply the western flank of the Alps (i.e., concave area) could play a role resulting in the enhancement or redistribution of rainfall. Thus, in order to better gauge the concave topography effects on the initiation and redistribution of orographic

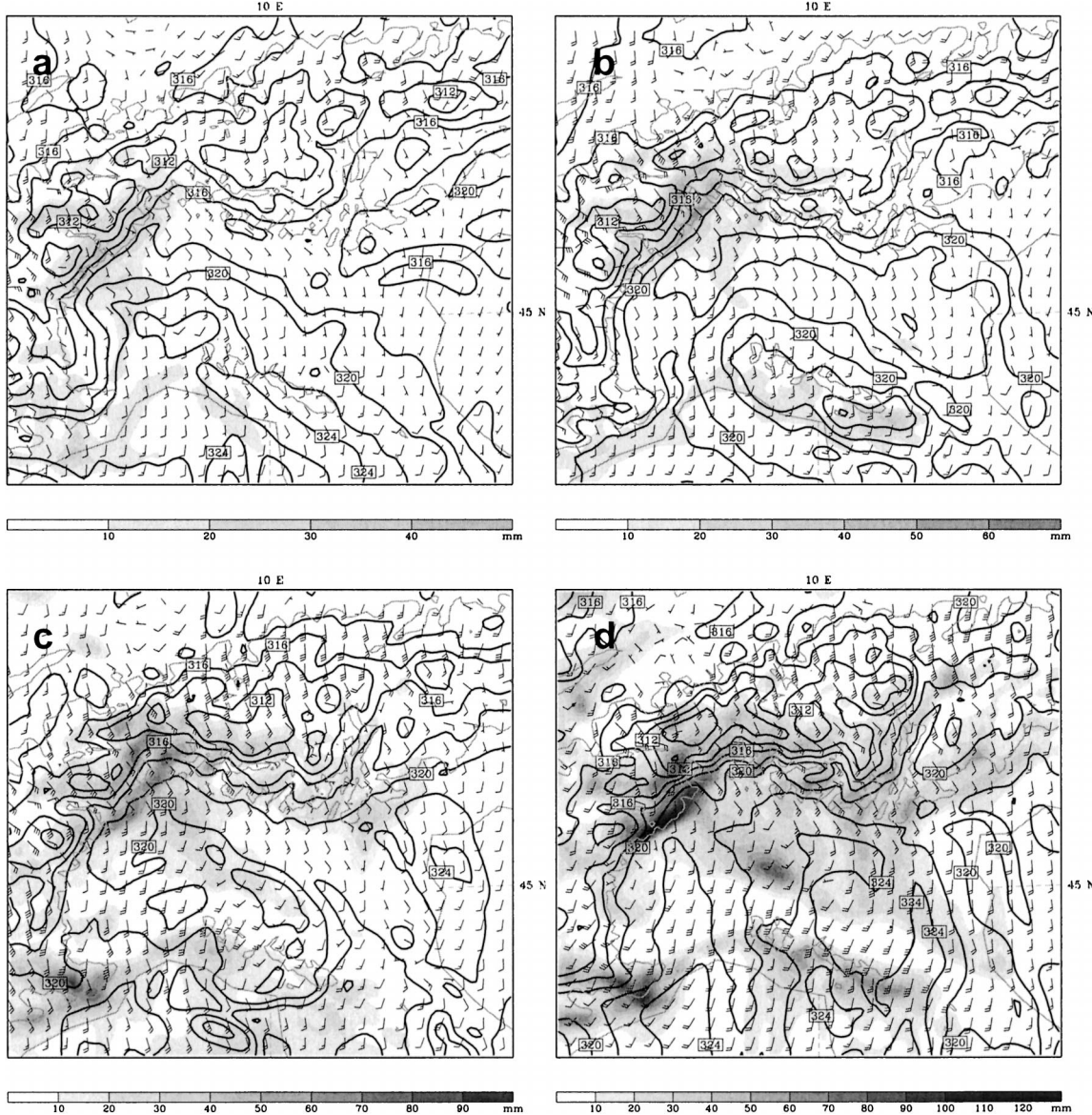


FIG. 10. Simulated 850-hPa winds (one full barb = 10 m s⁻¹), equivalent potential temperature (solid) every 3 K, and 6-h accumulated precipitation (shaded) from the 5-km-resolution NFRC case ending at (a) 1800 UTC 19 Sep, (b) 0000, (c) 0600, and (d) 1200 UTC 20 Sep 1999.

rainfall, we carried out an experiment in which the western flank of the Alps was set to be flat (approximately from 43° to 45°N), while keeping everything identical to the NAPN. The modified mountain was very similar to an elongated barrier-like obstacle (Fig. 9b). This experiment is referred to as the NWAP. From 1800 UTC 19 September to 0600 UTC 20 September, the wind field at 850 hPa was generally from the south. As shown in Fig. 14a, valid at 0600 UTC 20 September, the near-surface flow indicated a significant terrain-parallel barrier jet of ~10 m s⁻¹ from the Adriatic Sea. The low-level convergence was still along the Lago Maggiore area and the windward slopes. The westward turning of

the impinging southerly flow (~20 m s⁻¹) at 850 hPa occurred adjacent to the windward slopes of the Alps (Fig. 14c). A high θ_e (>324 K) zone was also present along the mountains. The precipitation distribution appears to be correlated with the slope areas of the modified mountains (i.e., the left end of the Alps). The maximum rainfall is located near the slope area of the Lago Maggiore region immediately aligned with the barrier jet.

By 1200 UTC 20 September (Figs. 14b and 14d), a clear cyclonic vortex existed along the left end of the modified mountains, where strong convergence was formed by the westerly and southeasterly flows. The

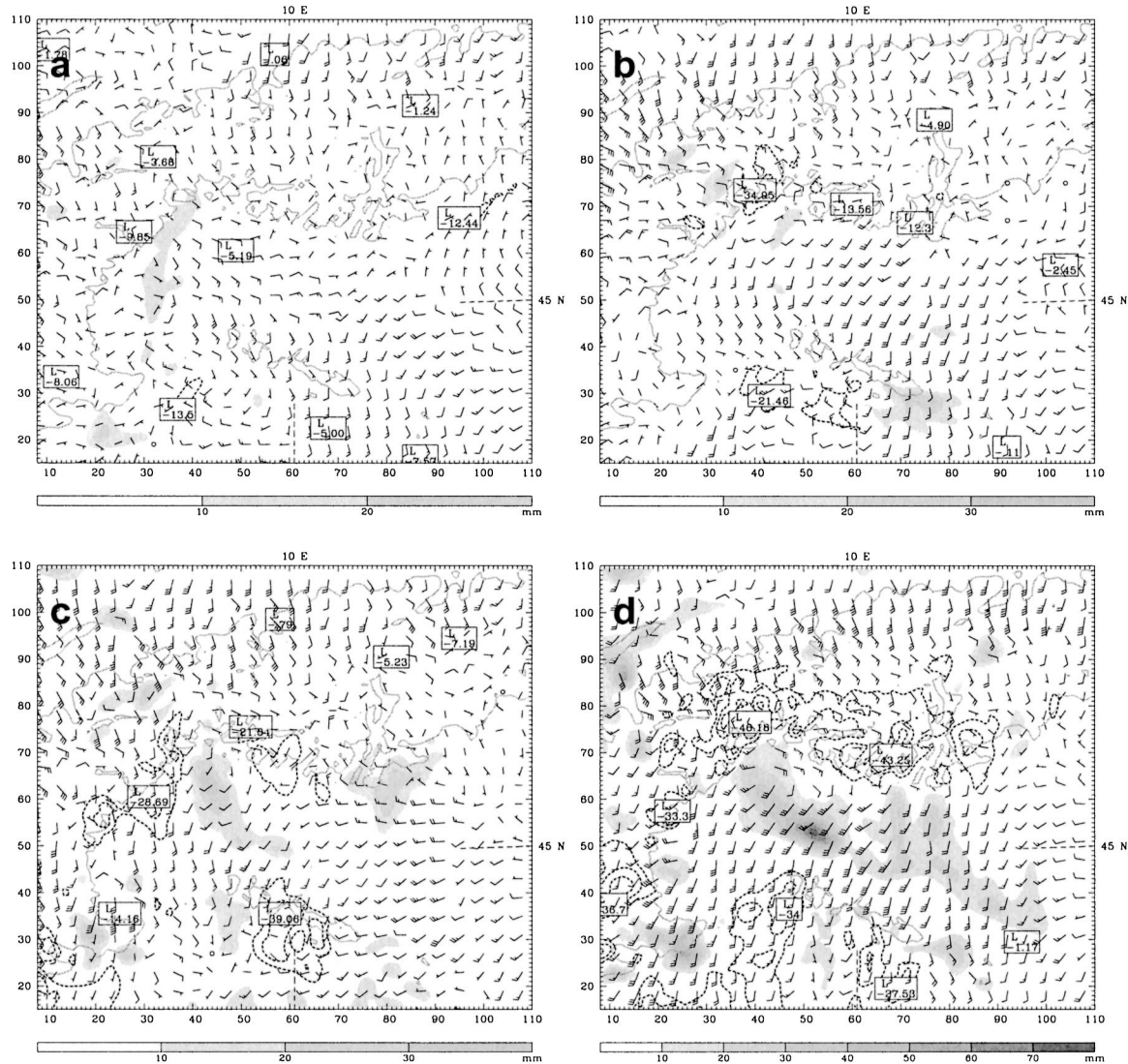


FIG. 11. Differences in the 6-h accumulated rainfall and wind field at surface level between the CTRL and NFRC experiments (NFRC - CTRL) at (a) 1800 UTC 19 Sep, (b) 0000, (c) 0600, and (d) 1200 UTC 20 Sep 1999 (positive: shaded; negative: dashed line).

model simulated a low pressure center at that area (not shown). Heavy rain was still concentrated on the windward slopes around the left end of the Alps. The 6-h simulated accumulated rainfall (~ 160 mm) was about 30 mm higher than NAPN and CTRL near the Lago Maggiore area from 0600 to 1200 UTC 20 September. The strong θ_e gradients were along the leading edge of westerly flow at this time (Fig. 14d). In addition, a narrow band of precipitation for the last 6 h (>70 mm) fell across the region in association with the trough that moved eastward to its present position. The precipitation amounts appear to be correlated with the steepest slopes at the left end of the mountains as well as the low pressure center. In comparison with the CTRL and NAPN cases (see Figs. 7 and 13), precipitation along the Lago Maggiore area remained strong. This result suggests that the French Alps do not play a significant

role in the formation of heavy rainfall near the Lago Maggiore area. This is consistent with the results of Buzzi et al. (1998) regarding the role of orography in the 1994 Piedmont flood case. In addition, the results also suggest that the type of flow regime (blocked) is apparent at the lower levels. These results again support the common ingredients concept of Lin et al. (2001a) for heavy orographic rainfall.

c. Effects of horizontal resolution

In order to study the effect of horizontal grid resolution on the orographic rainfall prediction, a sensitivity experiment was conducted using a horizontal grid size of 1.67 km (FALP). The initial condition was generated by one-way interpolation from the simulation results of the 5-km-resolution domain. The number of horizontal

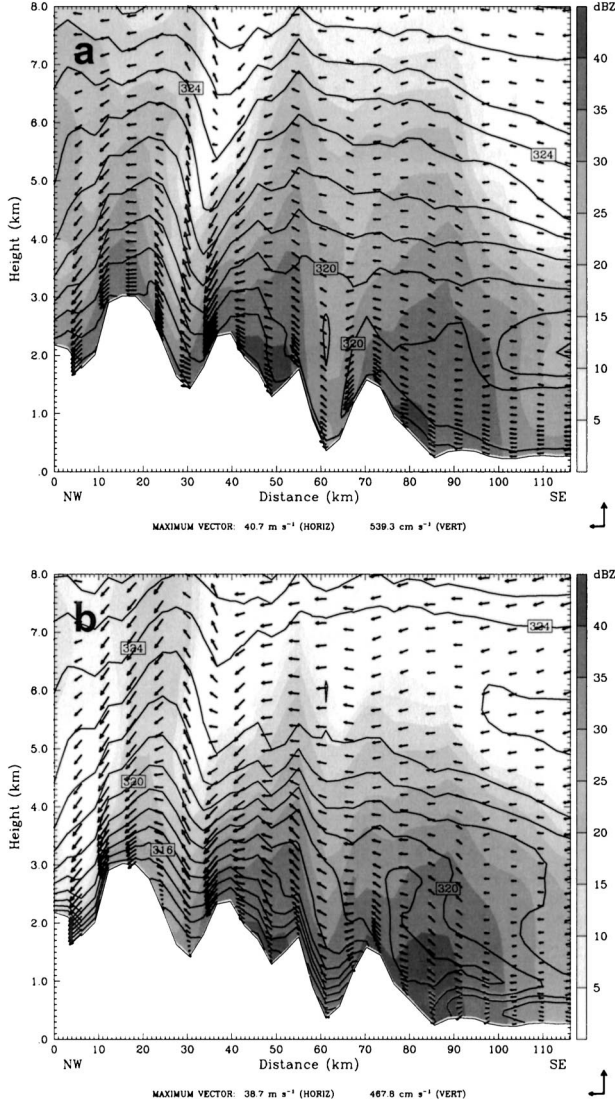


FIG. 12. Cross section AA' (see Fig. 1a) for the 5-km NFRC domain at (a) 0600 and (b) 1200 UTC 20 Sep 1999 showing equivalent potential temperatures (solid every 1 K), model reflectivities (shaded), and the total circulation (vectors) on the cross section.

grid points was 271×271 . The 1-km-resolution topography dataset was also used in this simulation. All other parameters in this experiment were identical to those in the CTRL except explicit cloud physics were used to replace the cumulus parameterization.

In the FALP experiment at 1800 UTC 19 September (Fig. 15a), a broad area of light precipitation developed along the French Alps. The simulated radar reflectivity along the cross section BB' indicated that convective echoes developed around the upslope region (Fig. 16a). The θ_e gradients and wind field were similar to those in the CTRL. As a result, from the decrease in horizontal grid length (increase in horizontal resolution), there was enhanced precipitation along the upslope region as compared to the CTRL (Fig. 7a). By 0000 UTC 20 Septem-

ber (Fig. 15b), heavy rainfall was concentrated near the Lago Maggiore area (>90 mm in 6 h). It was nearly 30 mm higher than the observed (Fig. 4b). Also, a narrow band of precipitation became aligned with the moist southerly low-level jet. Nevertheless, comparing Figs. 7b and 15b, the most striking difference was the broad precipitation area along the upslope region of the coastal Apennine Mountains in the CTRL, which was not that significant in this finer-resolution experiment. This was partly due to the topographic feature change in the coastal Apennine Mountains. Figure 16b shows a strong convective echo (>40 dBZ) structure over the first peak of the mountain range, where the impinging flow was approximately perpendicular to the upslope region. The simulated strong convective echo is similar to the observed analyses by S-Pol (cf. Fig. 1 in Houze and Medina 2001).

During the next 6 h (Fig. 15c), a noteworthy fact was that the model did reproduce the southerly low-level jet over the Gulf of Genoa in this simulation as compared to the ECMWF reanalysis (not shown), which was not well simulated in the CTRL run (Fig. 7c). However, the accumulated rainfall was overpredicted on the windward slopes of the Alps as well as the Maritime Alps. The rainfall was approximately 50% greater as compared to the CTRL simulation. A similar result was presented by Richard et al. (2002), in that the total precipitation was about 30% overestimated in their 2-km-resolution MM5 simulations. The cross section along the Lago Maggiore area showed that the upward motion (>3.2 m s $^{-1}$) was about twice as strong as the CTRL (not shown). As can be seen in Fig. 16c, a strong convective echo maximum appeared just upslope of the major rainfall cells over the terrain. The results suggested that vertical motion was further enhanced by the fine-resolution topography (i.e., steeper mountain slopes). The results also suggested that strong convective cells developed around each individual mountain peak. Caracena et al. (1979) proposed this idea to explain the low-altitude echo maximum in the orographic convective storm that produced the Big Thompson flood in the Rocky Mountains in 1976. In addition, Smith (1979) suggested that the convective cells can make the precipitation process faster and more efficient in broad-scale upslope flow. These small to moderate dBZ convective cells were associated with a deeper moisture layer, which affected the whole Alpine barrier. In other words, more moisture flow reached saturation over the windward slope than was deflected away from the barrier before condensation occurred.

At 1200 UTC 20 September (Fig. 15d), the windward slopes of the Alps were covered by broad-scale precipitation in FALP. Some heavy rainfall maxima were concentrated on the western side of the Lago Maggiore area. The location of these heavy rainfall maxima compared well with the rainfall accumulation as determined by S-Pol where amounts of over 275 mm were seen over specific peaks (see Fig. 25 in Houze 1999). As shown

0600 UTC 20

1200 UTC 20

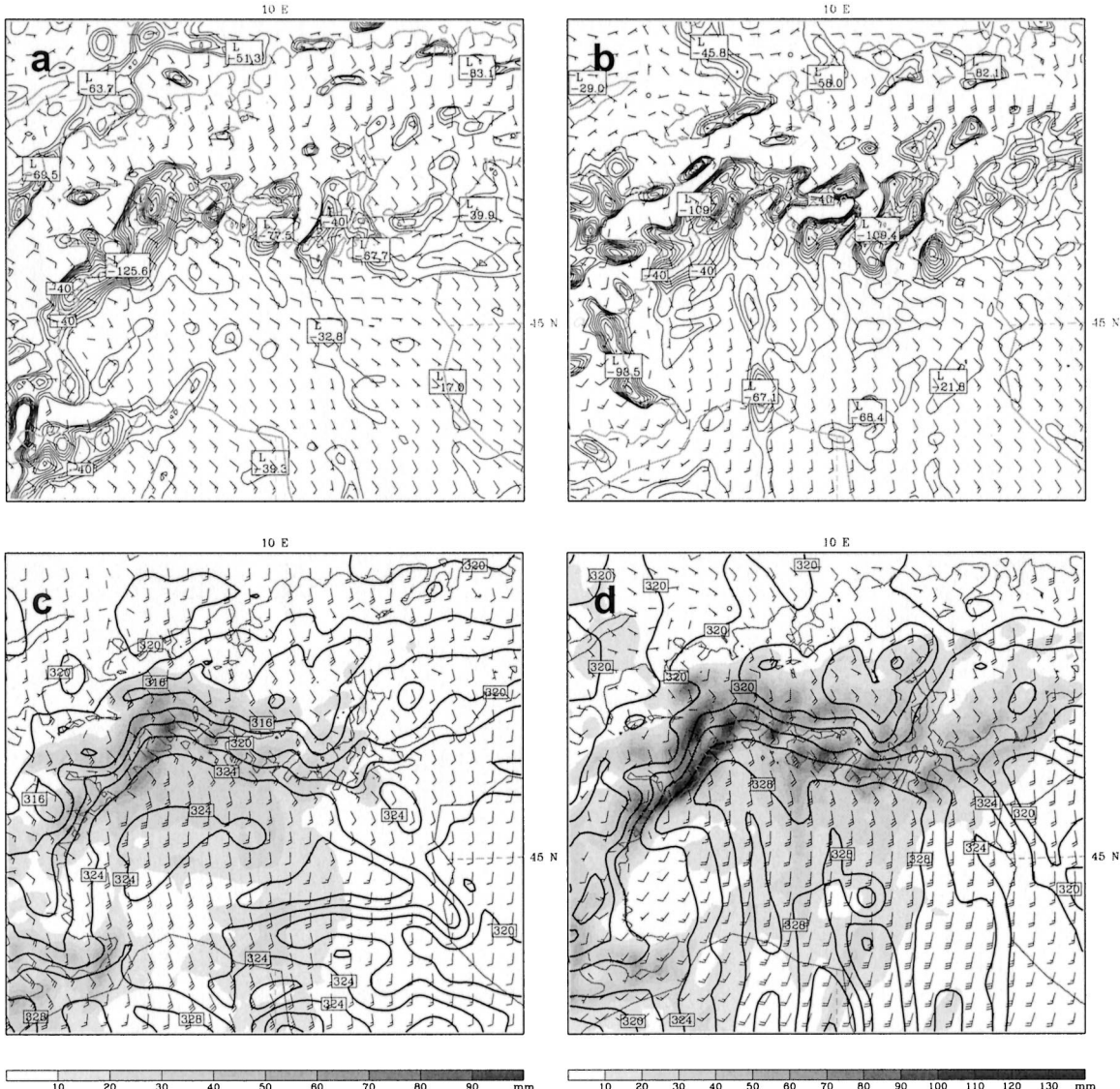


FIG. 13. Simulated surface level ($\sigma = 0.995$) wind field and convergence from the 5-km-resolution NAPN case at (a) 0600 and (b) 1200 UTC 20 Sep, and 850-hPa wind field and 6-h accumulated precipitation (shaded) ending at (c) 0600 and (d) 1200 UTC 20 Sep 1999 (one full barb = 10 m s^{-1}).

in Fig. 16d, the simulated radar reflectivity had increased in area coverage and intensity ($>45 \text{ dBZ}$) primarily because of the trough in association with the strong southerly low-level jet. Also, the convective echo was narrower in the presence of the mountains. Note that there was not much rain generated on the coastal Apennine Mountains during the entire heavy rainfall period. This was consistent with the observed rainfall analyses (Fig. 4). However, the model overpredicted the rainfall on the windward slopes of the Alps. In contrast, the CTRL produced a reasonable simulation of the rainfall amounts and distribution on the windward slopes

and in the Lago Maggiore area, but overpredicted the same over the coastal Apennine Mountains. A comparison of the time evolution of the hourly precipitation from the rain gauges over the 15-, 5-, and 1.67-km-resolution domains at Cimetta (46.2°N , 8.8°E ; station height: 1672 m) is shown in Fig. 17. The station is located in the Lago Maggiore area (as illustrated in Fig. 15a). Clearly, the increase in horizontal resolution has drastically changed the precipitation patterns and magnitudes and leads to an increase in precipitation, especially over the mountains. The results imply that the vertical motion increases rapidly as resolution increases,

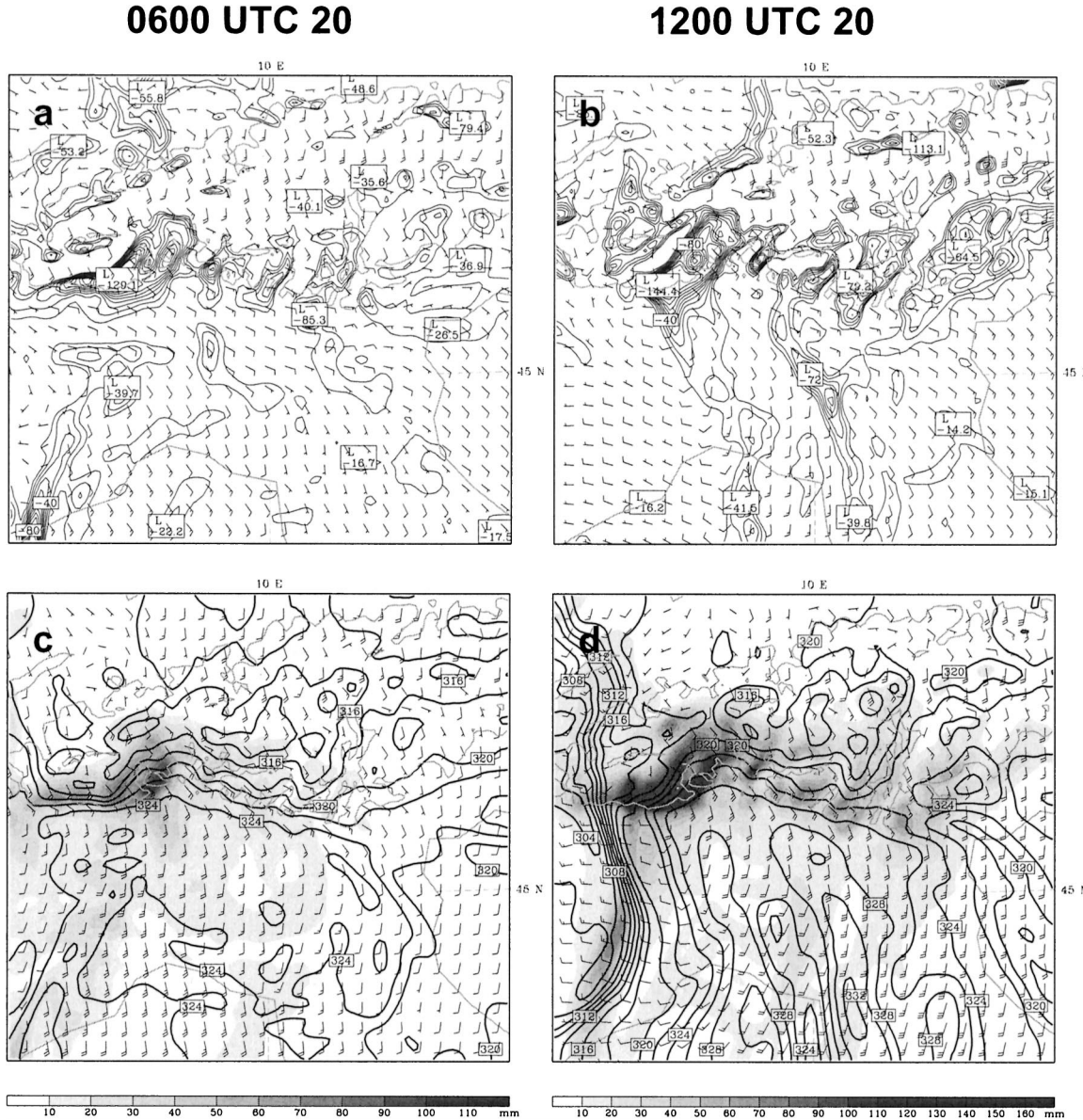


FIG. 14. Simulated surface level ($\sigma = 0.995$) wind field and convergence from the 5-km-resolution NWAP case at (a) 0600 and (b) 1200 UTC 20 Sep, and 850-hPa wind field, equivalent potential temperatures, and 6-h accumulated precipitation (shaded) ending at (c) 0600 and (d) 1200 UTC 20 Sep 1999 (one full barb = 10 m s^{-1}).

transitioning from less-than to greater-than particle fall speeds and allowing more variety of microphysical processes over complex topography. This may produce an extreme amount of precipitation. Colle et al. (2000) also demonstrated a similar result in their 4-km domain simulation over the Pacific Northwest. This rainfall over-prediction problem might be caused by the inaccurate or unrealistic parameterization of the microphysical processes over the steep mountains. Our results also suggest that improving the model's physical schemes might have the most significant impact on improving precipitation forecasts at higher resolutions, especially over the complex mountain areas.

6. Summary and discussion

This paper constitutes an extension of the previous work by Lin et al. (2001b), in which the synoptic and mesoscale environmental conditions were exploited to describe the evolution of a heavy orographic rainfall event in northern Italy during 19–21 September 1999 (MAP IOP-2B). During this event, the orographic precipitation was found to intensify rapidly as the deep trough approached the Alps. The goal of this study described here has been to use high-resolution mesoscale model simulations to investigate the local circulation and determine the responsible mechanisms for the heavy orographic precipitation.

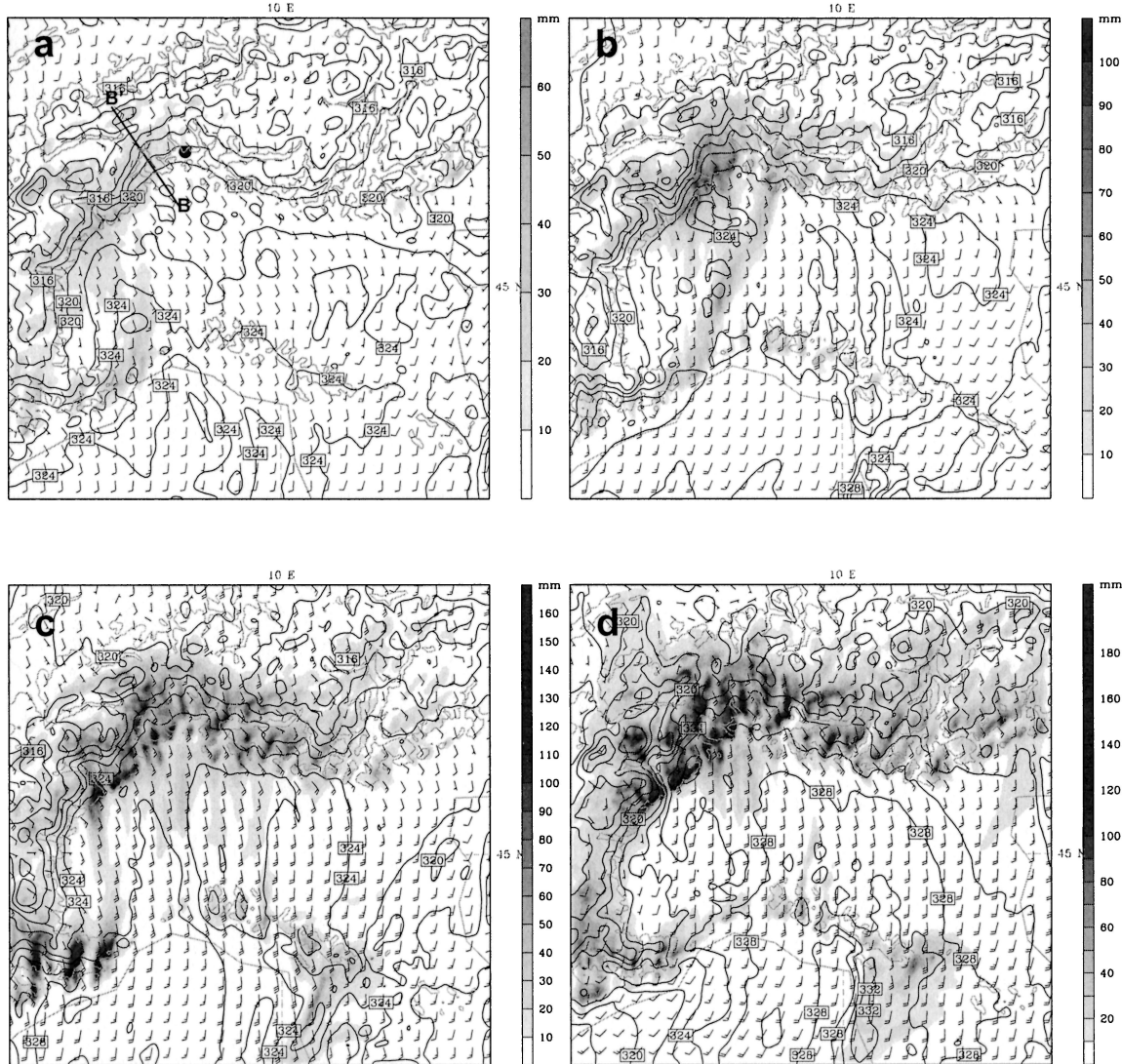


FIG. 15. Simulated 850-hPa winds (one full barb = 10 m s^{-1}), equivalent potential temperature (solid) every 3 K, and 6-h accumulated precipitation (shaded) from the 1.67-km-resolution FALP case ending at (a) 1800 UTC 19 Sep, (b) 0000, (c) 0600, and (d) 1200 UTC 20 Sep 1999. The solid line BB' represents the orientation of the x - z cross section in Fig. 16 analyses. Dot (●) point represents the surface station at Cimetta (46.2°N , 8.8°E).

This event was simulated with the PSU-NCAR Mesoscale Model at 5-km and finer horizontal resolution. Many of the major aspects of the precipitation event of IOP-2B were realistically reproduced, including the timing and location of rainfall. The moist flow into northern Italy at 850 hPa was generally from the south in association with high θ_e throughout the entire period of precipitation. The impinging moist flow was not substantially blocked by the barrier but rather easily flowed over the Alps. Most of the precipitation was found on the windward slopes in this event. The model results show good correspondence with major features in the observations. The surface flow (e.g., $\sigma = 0.995$) was characterized by a southerly jet from the Gulf of Genoa and an easterly jet from the Adriatic Sea. These two

flows impinged on the steep mountains near the Lago Maggiore region, which led to the development of strong convection along the steep mountain slopes. The westward deflection of the southerly flow occurred as it approached the barriers. The results are clearly discernible at the surface level. One notable weakness of the control simulation was that the 6-h accumulated rainfall was higher than was observed by as much as 30%, especially when the deep trough passed over the Lago Maggiore region. In spite of that, by examining the orographically induced vertical moisture flux and general vertical moisture flux (not shown), we found that the rainfall distribution over the mountains was roughly consistent with the orographically induced vertical moisture flux distribution. Convection enhanced by

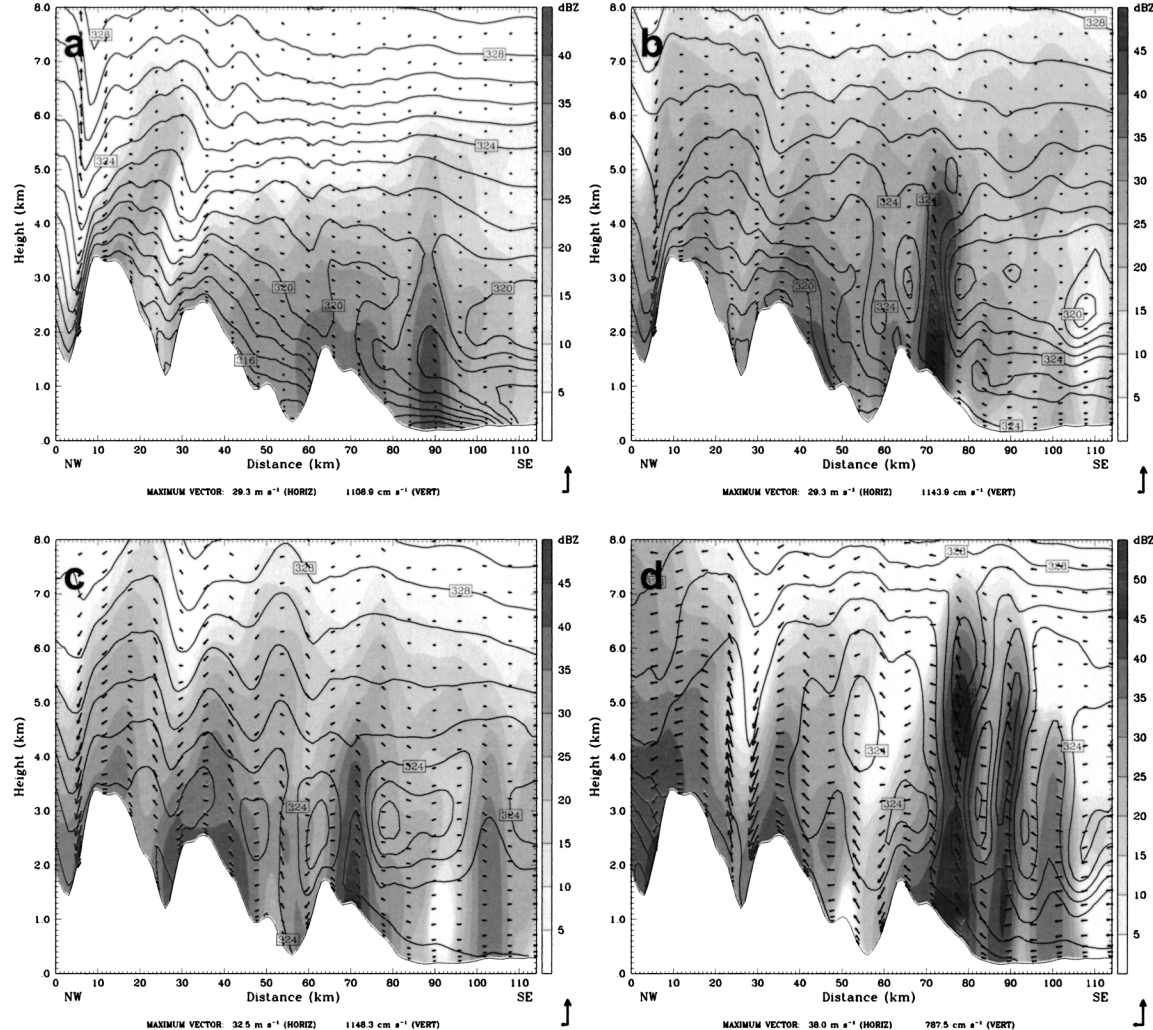


FIG. 16. Cross section BB' for the 1.67-km domain at (a) 1800 UTC 19 Sep, (b) 0000, (c) 0600, and (d) 1200 UTC 20 Sep 1999 showing equivalent potential temperatures (solid every 1 K), model reflectivities (shaded), and the total circulation (vectors) in the cross section.

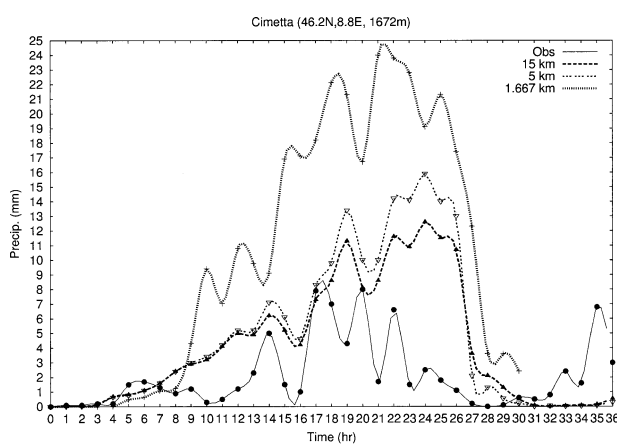


FIG. 17. Time evolution of the hourly precipitation as observed by the rain gauge, and as simulated with 15-, 5-, and 1.67-km domains at Cimetta (46.2°N , 8.8°E ; 1672 m).

orographic lifting plays an important role in such a heavy rainfall event, so forecasting the occurrence of deep convection is a critical part of any orographic precipitation event.

The control simulation and sensitivity experiments serve to illustrate the complex interrelationships among local circulation, complex topography, and precipitation distribution in northern Italy. The experiment without boundary layer friction (NFRC) reveals an important role of friction processes in the deflection of impinging southerly flow. In addition, more precipitation was produced in the lack of boundary layer friction condition, which was partly caused by the strong surface convergence. However, the convection was shallower because of the lack of boundary layer thermal fluxes. Our sensitivity test of the role of the Ligurian Apennine Mountains (NAPN) illustrated that the total amount and distribution of precipitation over the south side of the Alps was not directly affected by the

upstream mountains. However, this sensitivity experiment revealed a rain shadow effect resulting from downslope wind as the southerly wind flowed over the crest of the coastal Apennine Mountains. The sensitivity experiment on the existence of the French Alps (NWAP) indicates precipitation was concentrated along the steep slopes at the left end as well as the Lago Maggiore region of the mountains. A narrow-banded precipitation maximum was formed when the trough swept into northern Italy. This rainband was caused by the low-level convergence of velocity. Overall, the rainfall distribution over the Lago Maggiore region as well as the south side of the Alps was not significantly changed in either the absence of upstream mountains or the absence of the western flank of the Alps. The southerly flow at 850 hPa toward the Alps was moist and strong. A significant westward turning occurred at the surface level before the flow impinged on the barriers. Broad-scale precipitation fell on the Po Valley and the Piedmont areas in both experiments (i.e., NAPN and NWAP). Apparently, it is because of the lack of mountain blocking. The high-resolution experiment ($\delta x = 1.67$ km; FALP) illustrates that significant convective structure extended up to 7 km in the upslope regions. The results suggest that more intense convection is allowed to develop in the finer-resolution domain, which resulted in extremely heavy rainfall in the complex mountain areas, especially over the steeper upslope region. A comparison of precipitation from the observed analyses as well as the 15-, 5-, and 1.67-km domain simulations clearly illustrates that the increase in model resolution as well as the terrain resolution have drastically changed the precipitation patterns and magnitudes and leads to an overall increase in precipitation.

In general, this study illustrates that the orographically induced local circulation contributes to the formation and subsequent maintenance of a heavy orographic precipitation event in association with a deep trough approaching northern Italy. The finescale simulations reveal many important features of the local circulation, which includes flow deflection resulting from orographic blocking. In conclusion, the spatial and temporal distribution of orographic rainfall are reasonably simulated in the 5-km domain; however, the qualitatively evaluated orographic precipitation forecasts over complex topography still need to improve. To understand the interrelationships among the horizontal grid spacing, topographic resolution, and microphysical schemes, better turbulence closure schemes as well as better initial data are the keys to improve orographic precipitation forecasts.

Acknowledgments. We are very grateful to Drs. Simon Chang and Sethu Raman for their constructive comments and suggestions to improve this paper. Critical reviews of two anonymous reviewers have been very helpful. We also want to thank Dr. James A. Thurman

for proofreading the manuscript. This research is supported by the National Science Foundation Grant ATM-0096876. Computations are performed at the North Carolina Supercomputing Center and the National Center for Atmospheric Research.

REFERENCES

- Asencio, N., J. Stein, M. Chong, and F. Gheusi, 2003: Analysis and simulation of local and regional conditions for the rainfall over the Lago Maggiore target area during MAP IOP2B. *Quart. J. Roy. Meteor. Soc.*, **129**, 565–586.
- Bougeault, P., and Coauthors, 2001: The MAP special observing period. *Bull. Amer. Meteor. Soc.*, **82**, 433–462.
- Braun, S. A., R. Rotunno, and J. B. Klemp, 1999: Effects of coastal orography on landfalling cold fronts. Part II: Effects of surface friction. *J. Atmos. Sci.*, **56**, 3366–3384.
- Buzzi, A., and L. Foschini, 2000: Mesoscale meteorological features associated with heavy precipitation in the southern Alpine region. *Meteor. Atmos. Phys.*, **72**, 131–146.
- , N. Tartaglione, and P. Malguzzi, 1998: Numerical simulations of the 1994 Piedmont flood: Role of orography and moist processes. *Mon. Wea. Rev.*, **126**, 2369–2383.
- Caracena, F., R. A. Maddox, L. R. Hoxit, and C. F. Chappel, 1979: Mesoanalysis of the Big Thompson storm. *Mon. Wea. Rev.*, **107**, 1–17.
- Chen, C., C. H. Bishop, G. S. Lai, and W.-K. Tao, 1997: Numerical simulations of an observed narrow cold-frontal rainband. *Mon. Wea. Rev.*, **125**, 1027–1045.
- Chen, S.-H., and Y.-L. Lin, 2001: Orographic effects on a conditionally unstable flow over an idealized three-dimensional mesoscale mountain. MAP Newsletter, No. 15, MeteoSwiss, Zurich, Switzerland, 246–249.
- Colle, B. A., C. F. Mass, and K. J. Westrick, 2000: MM5 precipitation verification over the Pacific Northwest during the 1997–99 cool seasons. *Wea. Forecasting*, **15**, 730–744.
- Cressman, G. P., 1959: An operational objective analysis scheme. *Mon. Wea. Rev.*, **87**, 367–374.
- Dudhia, J., 1989: Numerical study of convection observed during the winter monsoon experiment using a mesoscale two-dimensional model. *J. Atmos. Sci.*, **46**, 3077–3107.
- Frei, C., 1995: An Alpine precipitation climatology based on high-resolution rain-gauge observations. MAP Newsletter, No. 3, MeteoSwiss, Zurich, Switzerland, 46–47.
- , cited 2004: Alpine precipitation analyses from high-resolution rain-gauge observations. Mesoscale Alpine Programme. [Available online at http://www.map.ethz.ch/map-doc/rr_clim.htm.]
- , and C. Schär, 1998: A precipitation climatology of the Alps from high-resolution rain-gauge observations. *Int. J. Climatol.*, **18**, 873–900.
- , and E. Häller, 2001: Mesoscale precipitation analysis from MAP SOP rain-gauge data. MAP Newsletter, No. 15, MeteoSwiss, Zurich, Switzerland, 257–260.
- Grell, G. A., J. Dudhia, and D. R. Stauffer, 1994: A description of the fifth-generation Penn State/NCAR Mesoscale Model (MM5). NCAR Tech. Note NCAR/TN-398+STR, 138 pp. [Available from National Center for Atmospheric Research, P. O. Box 3000, Boulder, CO 80307.]
- Houze, R., cited 1999: POC science director notes: IOP 02. [Available online at http://www.atmos.washington.edu/gcg/MG/MAP/summ/02/IOP_2B.991104.POC_sci.sumUW6B.html.]
- , and S. Medina, 2001: Alpine precipitation mechanisms in MAP IOP2b and 8. MAP Newsletter, No. 14, MeteoSwiss, Zurich, Switzerland, 3–5.
- , —, and M. Steiner, 2000: Two cases of heavy rain on the Mediterranean side of the Alps in MAP. Preprints, Ninth Conf. on Mountain Meteorology, Aspen, CO, Amer. Meteor. Soc., 1–5.
- Kain, J. S., and J. M. Fritsch, 1993: Convective parameterization for

- mesoscale models: The Kain–Fritsch scheme. *The Representation of Cumulus Convection in Numerical Models, Meteor. Monogr.*, No. 46, Amer. Meteor. Soc., 165–170.
- Kalnay, E., and Coauthors, 1996: The NCEP/NCAR 40-Year Reanalysis Project. *Bull. Amer. Meteor. Soc.*, **77**, 437–471.
- Klemp, J. B., and D. R. Durran, 1983: An upper boundary condition permitting internal gravity wave radiation in numerical mesoscale models. *Mon. Wea. Rev.*, **111**, 430–444.
- Lin, Y.-L., R. D. Farley, and H. D. Orville, 1983: Bulk parameterization of the snow field in a cloud model. *J. Climate Appl. Meteor.*, **22**, 40–63.
- , S. Chiao, T.-A. Wang, M. L. Kaplan, and R. P. Weglarz, 2001a: Some common ingredients for heavy orographic rainfall. *Wea. Forecasting*, **16**, 633–660.
- , J. A. Thurman, and S. Chiao, 2001b: Influence of synoptic and mesoscale environments on heavy orographic rainfall associated with MAP IOP-2B and IOP-8. MAP Newsletter, No. 15, MeteoSwiss, Zurich, Switzerland, 242–245.
- Medina, S., and R. A. Houze, 2003: Air motions and precipitation growth in Alpine storms. *Quart. J. Roy. Meteor. Soc.*, **129**, 345–372.
- Ólafsson, H., and P. Bougeault, 1997: The effect of rotation and surface friction on orographic drag. *J. Atmos. Sci.*, **54**, 193–210.
- Peng, M. S., J. H. Powell, R. T. Williams, and B. Jeng, 2001: Boundary layer effects on fronts over topography. *J. Atmos. Sci.*, **58**, 2222–2239.
- Ralph, F. M., P. J. Neiman, D. E. Kingsmill, E. D. Andrews, and R. C. Antweiler, 2003: The impact of a prominent rain shadow on flooding in California's Santa Cruz mountains: A CALJET case study and sensitivity to the ENSO cycle. *J. Hydrometeor.*, **4**, 1243–1264.
- Richard, E., P. Mascart, and E. C. Nickerson, 1989: The role of surface friction in downslope windstorms. *J. Appl. Meteor.*, **28**, 241–251.
- , and Coauthors, 2002: Intercomparison of the simulated precipitation fields of the MAP/IOP2b with different high-resolution models. Preprints, *10th Conf. on Mountain Meteorology and MAP Meeting 2002*, Park City, UT, Amer. Meteor. Soc., 167–170.
- Rotunno, R., and R. Ferretti, 2001: Mechanisms of intense Alpine rainfall. *J. Atmos. Sci.*, **58**, 1732–1749.
- , and —, 2002: Comparative analysis of rainfall in MAP cases IOP2B and IOP8. *Quart. J. Roy. Meteor. Soc.*, **128**, 373–390.
- Schneidereit, M., and C. Schär, 2000: Idealized numerical experiments of Alpine flow regimes and southside precipitation events. *Meteor. Atmos. Phys.*, **72**, 233–250.
- Smith, R. B., 1979: The influence of mountains on the atmosphere. *Advances in Geophysics*, Vol. 21, Academic Press, 87–230.
- , and S. Grønås, 1993: The 3-D mountain airflow bifurcation and the onset of flow splitting. *Tellus*, **45A**, 28–43.
- Smull, B., O. Bousquet, and M. Steiner, 2000: Contrasting stratification and mesoscale airflow in two heavy precipitation events observed during MAP. Preprints, *Ninth Conf. on Mountain Meteorology*, Aspen, CO, Amer. Meteor. Soc., 15–18.
- Stein, J., 2002: Moist airflow regimes over more or less smooth mountains. Preprints, *10th Conf. on Mountain Meteorology*, Park City, UT, Amer. Meteor. Soc., 178–181.
- Steiner, M., J. Smith, B. Smull, and R. Houze, 2000: Airflow within major river valleys on the south side of the Alps as observed during the MAP special observing period. Preprints, *Ninth Conf. on Mountain Meteorology*, Aspen, CO, Amer. Meteor. Soc., 11–14.
- Zhang, D., and R. A. Anthes, 1982: A high-resolution model of the planetary boundary layer-sensitivity tests and comparisons with SESAME-79 data. *J. Appl. Meteor.*, **21**, 1594–1609.